

Search for η and $\eta' \rightarrow \pi^+ e^- \bar{\nu}_e + c.c.$ decays in $J/\psi \rightarrow \phi\eta$ and $\phi\eta'$

M. Ablikim¹, M. N. Achasov⁶, O. Albayrak³, D. J. Ambrose³⁹, F. F. An¹, Q. An⁴⁰, J. Z. Bai¹, R. Baldini Ferroli^{17A}, Y. Ban²⁶, J. Becker², J. V. Bennett¹⁶, M. Bertani^{17A}, J. M. Bian³⁸, E. Boger^{19,a}, O. Bondarenko²⁰, I. Boyko¹⁹, R. A. Briere³, V. Bytev¹⁹, H. Cai⁴⁴, X. Cai¹, O. Cakir^{34A}, A. Calcaterra^{17A}, G. F. Cao¹, S. A. Cetin^{34B}, J. F. Chang¹, G. Chelkov^{19,a}, G. Chen¹, H. S. Chen¹, J. C. Chen¹, M. L. Chen¹, S. J. Chen²⁴, X. Chen²⁶, Y. B. Chen¹, H. P. Cheng¹⁴, Y. P. Chu¹, D. Cronin-Hennessy³⁸, H. L. Dai¹, J. P. Dai¹, D. Dedovich¹⁹, Z. Y. Deng¹, A. Denig¹⁸, I. Denysenko^{19,b}, M. Destefanis^{43A,43C}, W. M. Ding²⁸, Y. Ding²², L. Y. Dong¹, M. Y. Dong¹, S. X. Du⁴⁶, J. Fang¹, S. S. Fang¹, L. Fava^{43B,43C}, C. Q. Feng⁴⁰, P. Friedel², C. D. Fu¹, J. L. Fu²⁴, Y. Gao³³, C. Geng⁴⁰, K. Goetzen⁷, W. X. Gong¹, W. Gradl¹⁸, M. Greco^{43A,43C}, M. H. Gu¹, Y. T. Gu⁹, Y. H. Guan³⁶, N. G. Guler^{34A,34C,c}, A. Q. Guo²⁵, L. B. Guo²³, T. Guo²³, Y. P. Guo²⁵, Y. L. Han¹, F. A. Harris³⁷, K. L. He¹, M. He¹, Z. Y. He²⁵, T. Held², Y. K. Heng¹, Z. L. Hou¹, C. Hu²³, H. M. Hu¹, J. F. Hu³⁵, T. Hu¹, G. M. Huang⁴, G. S. Huang⁴⁰, J. S. Huang¹², L. Huang¹, X. T. Huang²⁸, Y. Huang²⁴, Y. P. Huang¹, T. Hussain⁴², C. S. Ji⁴⁰, Q. Ji¹, Q. P. Ji²⁵, X. B. Ji¹, X. L. Ji¹, L. L. Jiang¹, X. S. Jiang¹, J. B. Jiao²⁸, Z. Jiao¹⁴, D. P. Jin¹, S. Jin¹, F. F. Jing³³, N. Kalantar-Nayestanaki²⁰, M. Kavatsyuk²⁰, B. Kopf², M. Kornicer³⁷, W. Kuehn³⁵, W. Lai¹, J. S. Lange³⁵, M. Leyhe², C. H. Li¹, Cheng Li⁴⁰, Cui Li⁴⁰, D. M. Li⁴⁶, F. Li¹, G. Li¹, H. B. Li¹, J. C. Li¹, K. Li¹⁰, Lei Li¹, Q. J. Li¹, S. L. Li¹, W. D. Li¹, W. G. Li¹, X. L. Li²⁸, X. N. Li¹, X. Q. Li²⁵, X. R. Li²⁷, Z. B. Li³², H. Liang⁴⁰, Y. F. Liang³⁰, Y. T. Liang³⁵, G. R. Liao³³, X. T. Liao¹¹, D. Lin¹¹, B. J. Liu¹, C. L. Liu³, C. X. Liu¹, F. H. Liu²⁹, Fang Liu¹, Feng Liu⁴, H. Liu¹, H. B. Liu⁹, H. H. Liu¹³, H. M. Liu¹, H. W. Liu¹, J. P. Liu⁴⁴, K. Liu³³, K. Y. Liu²², Kai Liu³⁶, P. L. Liu²⁸, Q. Liu³⁶, S. B. Liu⁴⁰, X. Liu²¹, Y. B. Liu²⁵, Z. A. Liu¹, Zhiqiang Liu¹, Zhiqing Liu¹, H. Loehner²⁰, G. R. Lu¹², H. J. Lu¹⁴, J. G. Lu¹, Q. W. Lu²⁹, X. R. Lu³⁶, Y. P. Lu¹, C. L. Luo²³, M. X. Luo⁴⁵, T. Luo³⁷, X. L. Luo¹, M. Lv¹, C. L. Ma³⁶, F. C. Ma²², H. L. Ma¹, Q. M. Ma¹, S. Ma¹, T. Ma¹, X. Y. Ma¹, F. E. Maas¹¹, M. Maggiora^{43A,43C}, Q. A. Malik⁴², Y. J. Mao²⁶, Z. P. Mao¹, J. G. Messchendorp²⁰, J. Min¹, T. J. Min¹, R. E. Mitchell¹⁶, X. H. Mo¹, H. Moeini²⁰, C. Morales Morales¹¹, K. Moriya¹⁶, N. Yu. Muchnoi⁶, H. Muramatsu³⁹, Y. Nefedov¹⁹, C. Nicholson³⁶, I. B. Nikolaev⁶, Z. Ning¹, S. L. Olsen²⁷, Q. Ouyang¹, S. Pacetti^{17B}, J. W. Park²⁷, M. Pelizaeus², H. P. Peng⁴⁰, K. Peters⁷, J. L. Ping²³, R. G. Ping¹, R. Poling³⁸, E. Prencipe¹⁸, M. Qi²⁴, S. Qian¹, C. F. Qiao³⁶, L. Q. Qin²⁸, X. S. Qin¹, Y. Qin²⁶, Z. H. Qin¹, J. F. Qiu¹, K. H. Rashid⁴², G. Rong¹, X. D. Ruan⁹, A. Sarantsev^{19,d}, H. S. Sazak^{34A,34B,g}, B. D. Schaefer¹⁶, M. Shao⁴⁰, C. P. Shen^{37,e}, X. Y. Shen¹, H. Y. Sheng¹, M. R. Shepherd¹⁶, W. M. Song¹, X. Y. Song¹, S. Spataro^{43A,43C}, B. Spruck³⁵, D. H. Sun¹, G. X. Sun¹, J. F. Sun¹², S. S. Sun¹, Y. J. Sun⁴⁰, Y. Z. Sun¹, Z. J. Sun¹, Z. T. Sun⁴⁰, C. J. Tang³⁰, X. Tang¹, I. Tapan^{34C}, E. H. Thorndike³⁹, D. Toth³⁸, M. Ullrich³⁵, I. U. Uman^{34A,f}, G. S. Varner³⁷, B. Q. Wang²⁶, D. Wang²⁶, D. Y. Wang²⁶, K. Wang¹, L. L. Wang¹, L. S. Wang¹, M. Wang²⁸, P. Wang¹, P. L. Wang¹, Q. J. Wang¹, S. G. Wang²⁶, X. F. Wang³³, X. L. Wang⁴⁰, Y. D. Wang^{17A}, Y. F. Wang¹, Y. Q. Wang¹⁸, Z. Wang¹, Z. G. Wang¹, Z. Y. Wang¹, D. H. Wei⁸, J. B. Wei²⁶, P. Weidenkaff¹⁸, Q. G. Wen⁴⁰, S. P. Wen¹, M. Werner³⁵, U. Wiedner², L. H. Wu¹, N. Wu¹, S. X. Wu⁴⁰, W. Wu²⁵, Z. Wu¹, L. G. Xia³³, Y. X. Xia¹⁵, Z. J. Xiao²³, Y. G. Xie¹, Q. L. Xiu¹, G. F. Xu¹, G. M. Xu²⁶, Q. J. Xu¹⁰, Q. N. Xu³⁶, X. P. Xu³¹, Z. R. Xu⁴⁰, F. Xue⁴, Z. Xue¹, L. Yan⁴⁰, W. B. Yan⁴⁰, Y. H. Yan¹⁵, H. X. Yang¹, Y. Yang⁴, Y. X. Yang⁸, H. Ye¹, M. Ye¹, M. H. Ye⁵, B. X. Yu¹, C. X. Yu²⁵, H. W. Yu²⁶, J. S. Yu²¹, S. P. Yu²⁸, C. Z. Yuan¹, Y. Yuan¹, A. A. Zafar⁴², A. Zallo^{17A}, S. L. Zang²⁴, Y. Zeng¹⁵, B. Z. Zengin^{34A,34B,g}, B. X. Zhang¹, B. Y. Zhang¹, C. Zhang²⁴, C. C. Zhang¹, D. H. Zhang¹, H. H. Zhang³², H. Y. Zhang¹, J. Q. Zhang¹, J. W. Zhang¹, J. Y. Zhang¹, J. Z. Zhang¹, LiLi Zhang¹⁵, R. Zhang³⁶, S. H. Zhang¹, X. J. Zhang¹, X. Y. Zhang²⁸, Y. Zhang¹, Y. H. Zhang¹, Z. P. Zhang⁴⁰, Z. Y. Zhang⁴⁴, Zhenghao Zhang⁴, G. Zhao¹, H. S. Zhao¹, J. W. Zhao¹, K. X. Zhao²³, Lei Zhao⁴⁰, Ling Zhao¹, M. G. Zhao²⁵, Q. Zhao¹, S. J. Zhao⁴⁶, T. C. Zhao¹, X. H. Zhao²⁴, Y. B. Zhao¹, Z. G. Zhao⁴⁰, A. Zhemchugov^{19,a}, B. Zheng⁴¹, J. P. Zheng¹, Y. H. Zheng³⁶, B. Zhong²³, L. Zhou¹, X. Zhou⁴⁴, X. K. Zhou³⁶, X. R. Zhou⁴⁰, C. Zhu¹, K. Zhu¹, K. J. Zhu¹, S. H. Zhu¹, X. L. Zhu³³, Y. C. Zhu⁴⁰, Y. M. Zhu²⁵, Y. S. Zhu¹, Z. A. Zhu¹, J. Zhuang¹, B. S. Zou¹, J. H. Zou¹

(BESIII Collaboration)

¹ Institute of High Energy Physics, Beijing 100049, People's Republic of China

² Bochum Ruhr-University, D-44780 Bochum, Germany

³ Carnegie Mellon University, Pittsburgh, Pennsylvania 15213, USA

⁴ Central China Normal University, Wuhan 430079, People's Republic of China

⁵ China Center of Advanced Science and Technology, Beijing 100190, People's Republic of China

⁶ G.I. Budker Institute of Nuclear Physics SB RAS (BINP), Novosibirsk 630090, Russia

⁷ GSI Helmholtzcentre for Heavy Ion Research GmbH, D-64291 Darmstadt, Germany

⁸ Guangxi Normal University, Guilin 541004, People's Republic of China

⁹ GuangXi University, Nanning 530004, People's Republic of China

¹⁰ Hangzhou Normal University, Hangzhou 310036, People's Republic of China

¹¹ Helmholtz Institute Mainz, Johann-Joachim-Becher-Weg 45, D-55099 Mainz, Germany

¹² Henan Normal University, Xinxiang 453007, People's Republic of China

¹³ Henan University of Science and Technology, Luoyang 471003, People's Republic of China

¹⁴ Huangshan College, Huangshan 245000, People's Republic of China

¹⁵ Hunan University, Changsha 410082, People's Republic of China

¹⁶ Indiana University, Bloomington, Indiana 47405, USA

¹⁷ (A)INFN Laboratori Nazionali di Frascati, I-00044, Frascati,

Italy; (B)INFN and University of Perugia, I-06100, Perugia, Italy

¹⁸ Johannes Gutenberg University of Mainz, Johann-Joachim-Becher-Weg 45, D-55099 Mainz, Germany

- ¹⁹ Joint Institute for Nuclear Research, 141980 Dubna, Moscow region, Russia
- ²⁰ KVI, University of Groningen, NL-9747 AA Groningen, The Netherlands
- ²¹ Lanzhou University, Lanzhou 730000, People's Republic of China
- ²² Liaoning University, Shenyang 110036, People's Republic of China
- ²³ Nanjing Normal University, Nanjing 210023, People's Republic of China
- ²⁴ Nanjing University, Nanjing 210093, People's Republic of China
- ²⁵ Nankai University, Tianjin 300071, People's Republic of China
- ²⁶ Peking University, Beijing 100871, People's Republic of China
- ²⁷ Seoul National University, Seoul, 151-747 Korea
- ²⁸ Shandong University, Jinan 250100, People's Republic of China
- ²⁹ Shanxi University, Taiyuan 030006, People's Republic of China
- ³⁰ Sichuan University, Chengdu 610064, People's Republic of China
- ³¹ Soochow University, Suzhou 215006, People's Republic of China
- ³² Sun Yat-Sen University, Guangzhou 510275, People's Republic of China
- ³³ Tsinghua University, Beijing 100084, People's Republic of China
- ³⁴ (A)Ankara University, Dogol Caddesi, 06100 Tandogan, Ankara, Turkey; (B)Dogus University, 34722 Istanbul, Turkey; (C)Uludag University, 16059 Bursa, Turkey
- ³⁵ Universitaet Giessen, D-35392 Giessen, Germany
- ³⁶ University of Chinese Academy of Sciences, Beijing 100049, People's Republic of China
- ³⁷ University of Hawaii, Honolulu, Hawaii 96822, USA
- ³⁸ University of Minnesota, Minneapolis, Minnesota 55455, USA
- ³⁹ University of Rochester, Rochester, New York 14627, USA
- ⁴⁰ University of Science and Technology of China, Hefei 230026, People's Republic of China
- ⁴¹ University of South China, Hengyang 421001, People's Republic of China
- ⁴² University of the Punjab, Lahore-54590, Pakistan
- ⁴³ (A)University of Turin, I-10125, Turin, Italy; (B)University of Eastern Piedmont, I-15121, Alessandria, Italy; (C)INFN, I-10125, Turin, Italy
- ⁴⁴ Wuhan University, Wuhan 430072, People's Republic of China
- ⁴⁵ Zhejiang University, Hangzhou 310027, People's Republic of China
- ⁴⁶ Zhengzhou University, Zhengzhou 450001, People's Republic of China
- ^a Also at the Moscow Institute of Physics and Technology, Moscow 141700, Russia
- ^b On leave from the Bogolyubov Institute for Theoretical Physics, Kiev 03680, Ukraine
- ^c Currently at: Uludag University, Bursa, Turkey
- ^d Also at the PNPI, Gatchina 188300, Russia
- ^e Present address: Nagoya University, Nagoya 464-8601, Japan
- ^f Currently at: Dogus University, Istanbul, Turkey
- ^g Currently at: Ankara University, Ankara, Turkey
- (Dated: October 18, 2018)

Using a sample of 225.3 million J/ψ events collected with the BESIII detector at the BEPCII e^+e^- collider in 2009, searches for the decays of η and $\eta' \rightarrow \pi^+e^-\bar{\nu}_e + c.c.$ in $J/\psi \rightarrow \phi\eta$ and $\phi\eta'$ are performed. The ϕ signals, which are reconstructed in K^+K^- final states, are used to tag η and η' semileptonic decays. No signals are observed for either η or η' , and upper limits at the 90% confidence level are determined to be 7.3×10^{-4} and 5.0×10^{-4} for the ratios $\frac{\mathcal{B}(\eta \rightarrow \pi^+e^-\bar{\nu}_e + c.c.)}{\mathcal{B}(\eta \rightarrow \pi^+\pi^-\pi^0)}$ and $\frac{\mathcal{B}(\eta' \rightarrow \pi^+e^-\bar{\nu}_e + c.c.)}{\mathcal{B}(\eta' \rightarrow \pi^+\pi^-\eta)}$, respectively. These are the first upper limit values determined for η and η' semileptonic weak decays.

PACS numbers: 13.20.Gd, 14.40.Be, 13.20.Jf, 12.60.Cn

I. INTRODUCTION

Weak decays of quarkonium states such as η , η' , J/ψ and Υ , etc., offer a window into what may lie beyond the standard model (SM) [1–6]. The reason for the expected sensitivity is that the rates of the quarkonium weak decays are expected to be tiny in the framework of the SM [7]. As originally pointed out by Singer [8], the weak decays $\eta \rightarrow \pi^+l^-\bar{\nu}_l$ ($l = e, \mu$, and charge conjugate state implicitly included) are purely second class with a vector-type coupling in the

SM (see Ref. [9] for the definition of the second class current), and hence vanish in the limit of exact isospin symmetry. They occur in the SM in first order in the weak interaction, but only due to G -parity breaking effects, i.e. due to electromagnetic corrections and the mass-difference of the u - and d -quarks [10–17]. For η semileptonic weak decays, a one-loop calculation was performed in chiral perturbation theory within the SM, including a systematic treatment of the electromagnetic contributions to $O(e^2p^2)$ (e and p are electromagnetic coupling and typical momentum transfer in the decay as defined in Ref. [12]), and a rather accurate upper bound

for the branching fraction of $\eta \rightarrow \pi^+ l^- \bar{\nu}_l$ is predicted to be 2.6×10^{-13} . Therefore, any observation of $\eta \rightarrow \pi l \nu_l$ violating this bound would be a clear indication for new physics beyond the SM.

The decays $\eta \rightarrow \pi l \nu_l$ can be used to probe some types of possible new charged current interactions [10, 11]. A rather old suggestion would be the introduction of a new second class vector current for the $\eta \rightarrow \pi$ transition [15]. Scalar-type charged current four-fermion interactions can arise in gauge theories for example from the exchange of charged Higgs bosons in the two-Higgs-doublet model [18, 19]. Also light leptiquarks [20], occurring naturally in grand unified theories and composite models, may enhance the $\eta \rightarrow \pi l \nu_l$ branching fraction considerably [21]. For example, by considering scalar or vector type interaction, the branching fraction of $\eta \rightarrow \pi^+ l^- \bar{\nu}_l$ was estimated to be $10^{-8} - 10^{-9}$ [22, 23], which is a few order of magnitudes higher than that in the SM. Therefore, searches for the $\eta \rightarrow \pi^+ l^- \bar{\nu}_l$ and $\eta' \rightarrow \pi^+ l^- \bar{\nu}_l$ at the branching fractions level of $10^{-8} - 10^{-9}$ and below will provide information on the new physics beyond the SM. At present there is no experimental information on the decays $\eta \rightarrow \pi l \nu_l$. In this paper, we present measurements of branching fractions of η and $\eta' \rightarrow \pi^+ e^- \bar{\nu}_e$ decays. This analysis is based on $(225.3 \pm 2.8) \times 10^6 J/\psi$ events [24], accumulated with the Beijing Spectrometer III (BESIII) detector [25], at the Beijing Electron Positron Collider II (BEPCII).

II. THE BESIII EXPERIMENT AND MC SIMULATION

BEPCII/BESIII [25] is a major upgrade of the BESII experiment at the BEPC accelerator. The design peak luminosity of the double-ring e^+e^- collider, BEPCII, is $10^{33} \text{ cm}^{-2}\text{s}^{-1}$ at the center-of-mass energy of 3770 MeV. The BESIII detector has a geometrical acceptance of 93% of 4π and consists of four main components: (1) a small-celled, helium-based main drift chamber (MDC) with 43 layers, which provides measurements of ionization energy loss (dE/dx). The average single wire resolution is $135 \mu\text{m}$, and the momentum resolution for charged particles with momenta of 1 GeV/c in a 1 T magnetic field is 0.5%; (2) an electromagnetic calorimeter (EMC) made of 6240 CsI (Tl) crystals arranged in a cylindrical shape (barrel) plus two end-caps. For 1.0 GeV photons, the energy resolution is 2.5% in the barrel and 5% in the end-caps, and the position resolution is 6 mm in the barrel and 9 mm in the end-caps; (3) a time-of-flight system (TOF) for particle identification (PID) composed of a barrel part made of two layers with 88 pieces of 5 cm thick and 2.4 m long plastic scintillators in each layer, and two end-caps with 96 fan-shaped, 5 cm thick, plastic scintillators in each end-cap. The time resolution is 80 ps in the barrel, and 110 ps in the end-caps, corresponding to a 2σ K/ π separation for momenta up to about 1.0 GeV/c; (4) a muon chamber system made of 1000 m^2

of resistive-plate-chambers arranged in 9 layers in the barrel and 8 layers in the end-caps and incorporated in the return iron of the super-conducting magnet. The position resolution is about 2 cm.

The optimization of the event selection and the estimation of physics backgrounds are performed using Monte Carlo (MC) simulated data samples. The GEANT4-based simulation software BOOST [26] includes the geometric and material description of the BESIII detectors, the detector response and digitization models, as well as the track records of the detector running conditions and performance. The production of the J/ψ resonance is simulated by the MC event generator KKMC [27]; the known decay modes are generated by EVTGEN [28] with branching ratios taken from the Particle Data Group (PDG) tables [29] and determined by the Lundcharm model LUNDCHARM [30] for the remaining unknown decays. The analysis is performed in the framework of the BESIII offline software system [31] which takes care of the detector calibration, event reconstruction and data storage.

III. DATA ANALYSIS

A. Analyses for η and $\eta' \rightarrow \pi^+ e^- \bar{\nu}_e$

In order to detect η and $\eta' \rightarrow \pi^+ e^- \bar{\nu}_e$ decays, we use $J/\psi \rightarrow \phi\eta$ and $\phi\eta'$ decays. These two-body decays provide a very simple event topology, in which the ϕ signals can be reconstructed easily and cleanly decaying into K^+K^- . The reconstructed ϕ particles can be used to tag η and η' in order to allow a search for their semileptonic decays. In addition, the η and η' decays are easy to define in the lab system due to the strong boost of the ϕ from J/ψ decay.

Charged tracks in the BESIII detector are reconstructed using track-induced signals in the MDC. We select tracks within ± 10 cm of the interaction point in the beam direction and within 1 cm in the plane perpendicular to the beam direction. The tracks must be within the MDC fiducial volume, $|\cos\theta| < 0.93$ (θ is the polar angle with respect to the e^+ beam direction). Candidate events require four charged tracks with net charge zero. The TOF and dE/dx information are combined to form PID confidence levels for the π , K , and e hypotheses; each track is assigned to the particle type that corresponds to the hypothesis with the highest confidence level. To suppress background from $J/\psi \rightarrow \phi\eta$ (η'), where η (η') decays into nonleptonic modes, the electron candidate is further identified with the ratio of deposited energy in the EMC to track momentum, E/p , which must be larger than 0.8. We further require that E/p should be less than 0.8 for the pion candidate to suppress background from $J/\psi \rightarrow \phi\eta$ ($\eta \rightarrow \gamma e^+ e^-$) decay.

Showers identified as photon candidates must satisfy fiducial and shower-quality requirements. The minimum

energy is 25 MeV for EMC barrel showers ($|\cos\theta| < 0.8$) and 50 MeV for end-cap showers ($0.86 < |\cos\theta| < 0.92$). To eliminate showers produced by charged particles, a photon must be isolated from any charged track by more than 20° if not specified otherwise.

Since the mass of neutrino is almost zero and it is invisible in the detectors, a one-constraint (1C) kinematic fit is performed to constrain the missing mass of the reconstructed tracks to be zero, and $\chi^2_{1C} < 200$ is required. The 1C fit improves the resolution of recoil mass of the K^+K^- system by a factor of 2.5 for η case or a factor of 1.6 for η' case. After the 1C fit, the missing momentum $P_{\text{miss}} = |\vec{P}_{\text{miss}}|$ can be calculated; here, $\vec{P}_{\text{miss}} = -(\vec{P}_\phi + \vec{P}_{\pi^+} + \vec{P}_{e^-})$ in the rest frame of J/ψ , and we require that the missing momentum should be larger than 0.03 GeV/c to suppress backgrounds from final states with only four tracks, such as $J/\psi \rightarrow \phi\pi^+\pi^-$ ($\phi \rightarrow K^+K^-$). We count the number N_{shower} of EMC showers that could originate from a K_L or a photon, and require that N_{shower} be zero in the region inside a cone of 0.3 (1.5) rad around the direction of the missing momentum for $J/\psi \rightarrow \phi\eta(\eta')$ [$\eta(\eta') \rightarrow \pi^+e^-\bar{\nu}_e$]. These requirements reject most η and η' decays into nonleptonic final states. They also eliminate most backgrounds from multi-body decays of $J/\psi \rightarrow \phi + \text{anything}$. The different requirements on the cone angle for the η and η' cases are made because of the following two reasons: firstly, in the $J/\psi \rightarrow \phi\eta(\eta')$ decays, the booster for η is stranger than that for η' in the central of mass energy of J/ψ , which leads to a larger open angle for the η' decay products than that for the η decay products in the detector. Secondly, the most dangerous backgrounds are from $\eta(\eta') \rightarrow \pi^+\pi^-\gamma$ decay, in which one of the charged pions is mis-identified as an electron. Meanwhile, the decay rate for $\eta' \rightarrow \pi^+\pi^-\gamma$ is more than 6 times larger than the rate for $\eta \rightarrow \pi^+\pi^-\gamma$ [29].

Figures 1 (a) and (b) show the invariant mass distribution of K^+K^- candidates, $m_{K^+K^-}$, after the above selections. Clear ϕ signals are seen. The invariant mass of $\pi^+e^-\bar{\nu}_e$ can be obtained as $m_{\pi^+e^-\bar{\nu}_e} = \sqrt{(E_{\pi^+} + E_{e^-} + E_{\bar{\nu}_e})^2 - (\vec{P}_{\pi^+} + \vec{P}_{e^-} + \vec{P}_{\bar{\nu}_e})^2}$, where $E_{\bar{\nu}_e} \equiv E_{\text{miss}} = |\vec{P}_{\text{miss}}|$ and $\vec{P}_{\bar{\nu}_e} = \vec{P}_{\text{miss}}$. Figures 2 (a) and (b) show the $m_{\pi^+e^-\bar{\nu}_e}$ distributions for events with $1.01 < m_{K^+K^-} < 1.03$ GeV/c² for the decays $J/\psi \rightarrow \phi\eta$ ($\eta \rightarrow \pi^+e^-\bar{\nu}_e$) and $J/\psi \rightarrow \phi\eta'$ ($\eta' \rightarrow \pi^+e^-\bar{\nu}_e$), respectively. No events are observed in the η and η' signal regions. The signal regions for η and η' are defined in the ranges [0.51, 0.58] and [0.92, 0.99] GeV/c², respectively, on the mass of $\pi^+e^-\bar{\nu}_e$.

We use MC simulated events to determine selection efficiencies for the signal channels and study possible backgrounds. With phase space MC simulations, we obtain efficiencies of 17.9% and 17.4% for η and η' semileptonic decays, respectively. According to the study of the J/ψ inclusive MC sample, more than 20 exclusive decay modes are identified as potential background modes, and are studied with full MC simulations in

order to understand the backgrounds. The sources of backgrounds are divided into two classes. Class I: The background is from $J/\psi \rightarrow \phi\eta(\eta')$, $\phi \rightarrow K^+K^-$ and η (η') decays into other modes than the signal final states. We find that the expected number of background events from this class is 0.18 ± 0.05 (0.58 ± 0.09) in the signal region for η (η'). Class II: It is mainly from J/ψ decays to the final states without η or η' , such as $\phi\pi^+\pi^-$, $\phi f_0(980)$ ($f_0(980) \rightarrow \pi^+\pi^-$), and $K^{*0}\bar{K}^{*0}$ ($K^{*0} \rightarrow K^\pm\pi^\mp$). The expected number of background events from class II is 0.05 ± 0.04 (0.45 ± 0.13) in the signal region for the η (η') case. The total number of background events is 0.23 ± 0.06 (1.03 ± 0.16) in the signal region for η (η').

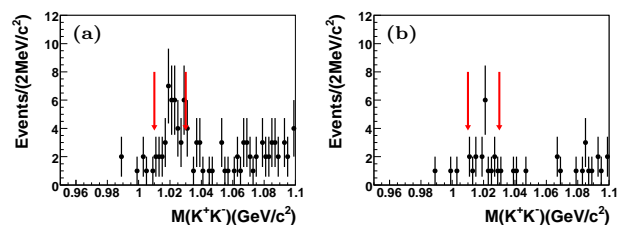


FIG. 1: The $m_{K^+K^-}$ distributions of candidate events: (a) for $J/\psi \rightarrow \phi\eta$; (b) for $J/\psi \rightarrow \phi\eta'$. The arrows on the plots indicate the signal region of ϕ candidates.

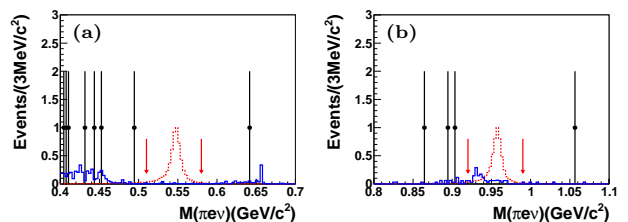


FIG. 2: The $m_{\pi^+e^-\bar{\nu}_e}$ distributions of candidate events: (a) for $J/\psi \rightarrow \phi\eta$ ($\eta \rightarrow \pi^+e^-\bar{\nu}_e$); (b) for $J/\psi \rightarrow \phi\eta'$ ($\eta' \rightarrow \pi^+e^-\bar{\nu}_e$). For both (a) and (b): the data (dots with error bars) are compared to the signal MC samples (red dashed histogram) and the expected backgrounds (solid blue histogram). The arrows on the plots indicate the signal regions of η and η' candidates.

After all selection criteria are applied, no event survives in the η and η' signal regions. The signal components and the expected background shapes are projected and compared to data for both η and η' cases, as shown in Figs. 2 (a) and (b). We set an upper limit at the 90% confidence level (C.L.) to be $N_{\text{UL}}^\eta = 2.36$ ($N_{\text{UL}}^{\eta'} = 1.59$) for $\eta(\eta')$, using the POLE⁺⁺ program [32] with the Feldman-Cousins frequentist approach [33]. The information used to obtain the upper limit includes the number of observed events in the signal region, and the expected number of background events and their uncertainty.

B. Analyses for η (η') $\rightarrow \pi^+\pi^-\pi^0(\eta)$

The $\eta \rightarrow \pi^+\pi^-\pi^0$ and $\eta' \rightarrow \pi^+\pi^-\eta$ decays are also studied in $J/\psi \rightarrow \phi\eta$ and $\phi\eta'$ processes, in order to obtain the ratio of $\mathcal{B}(\eta(\eta') \rightarrow \pi^+e^-\bar{\nu}_e + c.c.)$ to $\mathcal{B}(\eta \rightarrow \pi^+\pi^-\pi^0)$ ($\mathcal{B}(\eta \rightarrow \pi^+\pi^-\eta)$). The advantage of measuring the ratios of semileptonic weak decays over hadronic decays $\frac{\mathcal{B}(\eta \rightarrow \pi^+e^-\bar{\nu}_e + c.c.)}{\mathcal{B}(\eta \rightarrow \pi^+\pi^-\pi^0)}$ and $\frac{\mathcal{B}(\eta' \rightarrow \pi^+e^-\bar{\nu}_e + c.c.)}{\mathcal{B}(\eta' \rightarrow \pi^+\pi^-\eta)}$ is that the uncertainties due to the total number of J/ψ events, tracking efficiency, PID for kaon and one pion, the number of the charged tracks, and residual noise in the EMC cancel.

The selection criteria for the charged tracks are the same as those for the $J/\psi \rightarrow \phi\eta$ (η'), η (η') $\rightarrow \pi^+e^-\bar{\nu}_e$ decays except for the electron identification requirement. The candidate events are required to have two charged kaons and two charged pions with opposite charge. In addition, two photon candidates are required to reconstruct $\pi^0 \rightarrow \gamma\gamma$ and $\eta \rightarrow \gamma\gamma$ in the $\eta \rightarrow \pi^+\pi^-\pi^0$ and $\eta' \rightarrow \pi^+\pi^-\eta$ decays, respectively. The photon candidates are required to be isolated from all charged tracks by more than 10° which is different from the selection criteria for the $J/\psi \rightarrow \phi\eta$ (η'), η (η') $\rightarrow \pi^+e^-\bar{\nu}_e$ decays in order to improve the efficiency of $\pi^0(\eta)$ reconstruction. A four-constraint (4C) energy-momentum conservation kinematic fit is performed to the $J/\psi \rightarrow K^+K^-\pi^+\pi^-\gamma\gamma$ hypothesis, and only events with $\chi_{4C}^2 < 200$ are accepted. For events with more than two photon candidates, the combination with the minimum χ_{4C}^2 is selected. After the 4C fits, the π^0 and η signal windows on the $\gamma\gamma$ invariant mass distributions are defined in the ranges $0.115 < m_{\gamma\gamma} < 0.150$ GeV/ c^2 and $0.518 < m_{\gamma\gamma} < 0.578$ GeV/ c^2 , respectively.

The numbers of $J/\psi \rightarrow \phi\eta$ (η'), η (η') $\rightarrow \pi^+\pi^-\pi^0(\eta)$ events are obtained from an unbinned extended maximum likelihood (ML) fit to the K^+K^- versus $\pi^+\pi^-\pi^0(\eta)$ invariant mass distributions. The projection of the fit on the m_{KK} ($m_{\pi^+\pi^-\pi^0}$ and $m_{\pi^+\pi^-\eta}$) axis is shown in Figs. 3 (a) and 4 (a) [Figs. 3 (b) and 4 (b)] for the η and η' cases, respectively. In the ML fits, we require that 0.99 GeV/ $c^2 < m_{KK} < 1.09$ GeV/ c^2 and 0.50 GeV/ $c^2 < m_{\pi^+\pi^-\pi^0} < 0.60$ GeV/ c^2 (0.87 GeV/ $c^2 < m_{\pi^+\pi^-\eta} < 1.07$ GeV/ c^2) for the η (η') case. The signal shape for ϕ is modeled with a relativistic Breit-Wigner (RBW) function [34] convoluted with a Gaussian function that represents the detector resolution. In the fit, the width of ϕ is fixed at the PDG value, and its central mass value is floated, and the width of the Gaussian is free; the signal shape for η (η') is described by a Crystal Ball (CB) function [35], and its parameters are floated. The backgrounds are divided into three categories: non- $\phi\eta(\eta')$ -peaking background (*i.e.*, $J/\psi \rightarrow \pi^+\pi^-\pi^0K^+K^-$); non- ϕ -peaking background [*i.e.*, $J/\psi \rightarrow K^+K^-\eta$ (η')]; and non- $\eta(\eta')$ -peaking background (*i.e.*, $J/\psi \rightarrow \phi\pi^+\pi^-\pi^0$). The probability density functions (PDF) for non- ϕ -peaking background

in the m_{KK} distribution is parameterized by [36]

$$B(m_{KK}) = (m_{KK} - 2m_K)^a \cdot e^{-bm_{KK} - cm_{KK}^2}, \quad (1)$$

where a , b and c are free parameters, and m_K is the nominal mass value of the charged kaon from the PDG [29]. The shape for the non- $\eta(\eta')$ -peaking background in the $m_{\pi^+\pi^-\pi^0(\eta)}$ distribution is modeled by a first-order Chebychev polynomial function [$B(m_{\pi^+\pi^-\pi^0(\eta)})$]. All parameters related to the background shape are floated in the fit to data. Totally, 14 parameters including signal and background yields are floated in the fit. The PDFs for signal and backgrounds are combined in the likelihood function \mathcal{L} , defined as a function of the free parameters N^η , $N_{\text{bkg}}^{\text{non-}\phi\eta}$, $N_{\text{bkg}}^{\text{non-}\phi}$, and $N_{\text{bkg}}^{\text{non-}\eta}$:

$$\begin{aligned} \mathcal{L} = & \frac{e^{-(N^\eta + N_{\text{bkg}}^{\text{non-}\phi\eta} + N_{\text{bkg}}^{\text{non-}\phi} + N_{\text{bkg}}^{\text{non-}\eta})}}{N!} \\ & \times \prod_{i=1}^N [N^\eta \text{RBW}(m_{KK}^i) \times \text{CB}(m_{\pi^+\pi^-\pi^0}^i) \\ & + N_{\text{bkg}}^{\text{non-}\phi\eta} B(m_{KK}^i) \times B(m_{\pi^+\pi^-\pi^0}^i) \\ & + N_{\text{bkg}}^{\text{non-}\phi} B(m_{KK}^i) \times \text{CB}(m_{\pi^+\pi^-\pi^0}^i) \\ & + N_{\text{bkg}}^{\text{non-}\eta} \text{RBW}(m_{KK}^i) \times B(m_{\pi^+\pi^-\pi^0}^i)], \quad (2) \end{aligned}$$

where N^η is the number of $J/\psi \rightarrow \phi\eta$, $\phi \rightarrow K^+K^-$, $\eta \rightarrow \pi^+\pi^-\pi^0$ events, and $N_{\text{bkg}}^{\text{non-}\phi\eta}$, $N_{\text{bkg}}^{\text{non-}\phi}$, and $N_{\text{bkg}}^{\text{non-}\eta}$ are the numbers of the corresponding three kinds of backgrounds. The fixed parameter N is the total number of selected events in the fit region, and m_{KK}^i ($m_{\pi^+\pi^-\pi^0}^i$) is the value of m_{KK} ($m_{\pi^+\pi^-\pi^0}$) for the i th event. We use the product of the PDFs, since we have verified that m_{KK} and $m_{\pi^+\pi^-\pi^0}$ are uncorrelated for each component. The negative log-likelihood ($-\ln\mathcal{L}$) is then minimized with respect to the extracted yields. The resulting fitted signal and background yields are summarized in Table I. We also obtain the results for the η' case by replacing η and π^0 with η' and η in Eq. (2). The fitted results for η (η') $\rightarrow \pi^+\pi^-\pi^0(\eta)$ are shown in Fig. 3 (Fig. 4). The detection efficiencies are determined with MC simulations to be 20.37% and 20.89% for η and η' , respectively.

IV. SYSTEMATIC UNCERTAINTIES

Contributions to the systematic error on the ratios are summarized in Table II. The uncertainty, due to the requirement of no neutral showers in the EMC inside a cone spanning 0.3 (1.5) rad around the direction of the missing momentum for η (η') decay is obtained using the control sample of decays $J/\psi \rightarrow \phi\eta'$, $\phi \rightarrow K^+K^-$, $\eta' \rightarrow \gamma\pi^+\pi^-$. We calculated the missing momentum of the $K^+K^-\pi^+\pi^-$ system, and define the same cones around the direction of the missing momentum as in the η

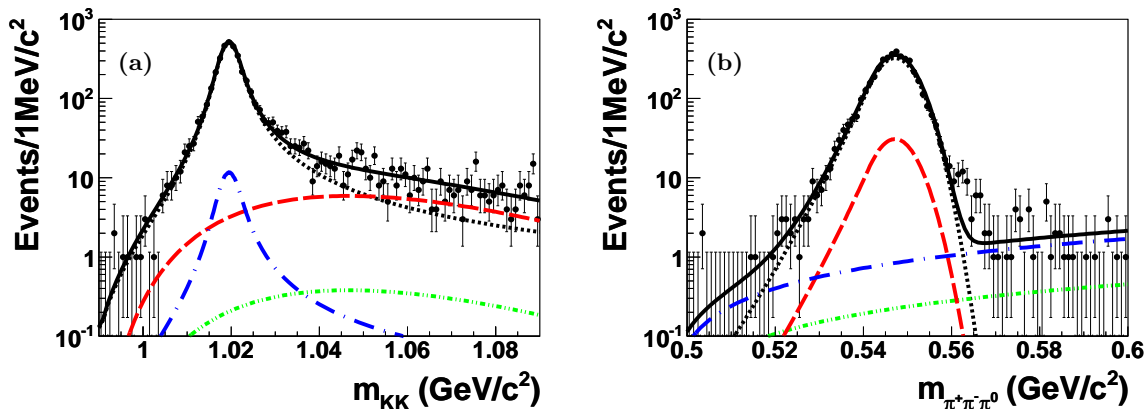


FIG. 3: The (a) m_{KK} and (b) $m_{\pi^+\pi^-\pi^0}$ distributions with fit results superimposed for $J/\psi \rightarrow \phi\eta$, $\phi \rightarrow K^+K^-$, $\eta \rightarrow \pi^+\pi^-\pi^0$. Points with error bars are data. The (black) solid curves show the results of the total fits, and the (black) short-dashed curves are for signals. The (blue) dotted-dash curve shows non- η -peaking backgrounds, the (red) dashed curve shows the non- ϕ -peaking background, and the (green) dotted-short-dash curve shows non- $\phi\eta$ -peaking backgrounds.

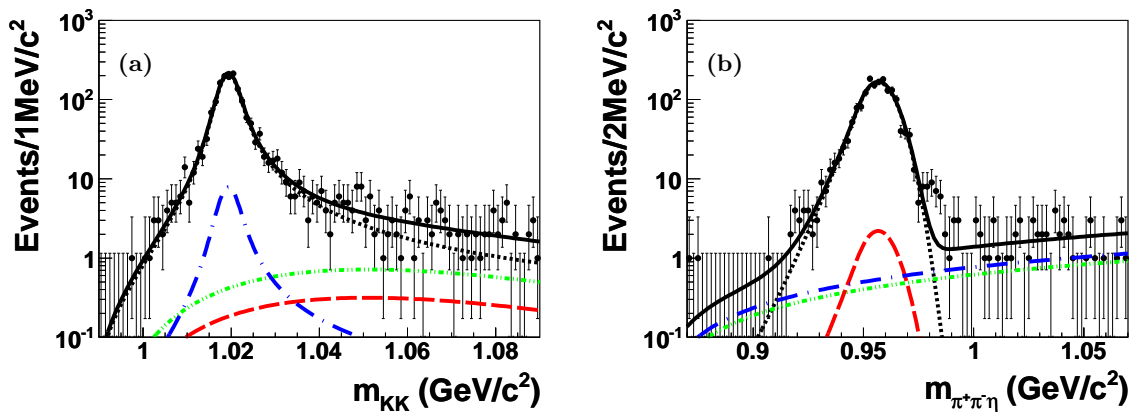


FIG. 4: The (a) m_{KK} and (b) $m_{\pi^+\pi^-\eta}$ distributions with fit results superimposed for $J/\psi \rightarrow \phi\eta'$, $\phi \rightarrow K^+K^-$, $\eta' \rightarrow \pi^+\pi^-\eta$. Points with error bars are data. The (black) solid curves show the results of the total fits, and the (black) short-dashed curves are for signals. The (blue) dotted-dash curve shows non- η' -peaking backgrounds, the (red) dashed curve shows the non- ϕ -peaking background, and the (green) dotted-short-dash curve shows non- $\phi\eta'$ -peaking backgrounds.

(η') semileptonic analysis. The ratios of events with the requirement on the number of extra photons to events without the requirement are obtained for both data and MC simulation. The difference 0.1% (1.1%) is considered as a systematic error for the η (η') case.

We also use the control sample of $J/\psi \rightarrow \phi\eta'$, $\phi \rightarrow K^+K^-$, $\eta' \rightarrow \gamma\pi^+\pi^-$ to obtain the uncertainty due to the requirement on the missing momentum $P_{\text{miss}} > 0.03$ GeV/ c for both η and η' cases. Thus we calculated the missing momentum of the $K^+K^-\pi^+\pi^-$ system. The ratios of events with the requirement on the missing momentum $P_{\text{miss}} > 0.03$ GeV/ c to events without the requirement are obtained for both data and MC simulation. The difference 2.5% is considered as a systematic error for both η and η' cases.

The phase space MC is used to generate η (η') \rightarrow

$\pi^+e^-\bar{\nu}_e$ decays. In Ref. [12], the transition form factors $f_{\pm}^{\eta\pi}$ are calculated at the one-loop level in the chiral perturbation theory. We use the model predictions to generate signal MC events, and find that the uncertainty on the detection efficiency is changed by 1.0% (5.0%) for the η (η') case.

Since the uncertainties on the PID of the electron and one of the pions do not cancel in the ratio, the efficiencies for pion and electron PID are obtained with the control samples of $J/\psi \rightarrow \pi^+\pi^-\pi^0$ and radiative Bhabha scattering $e^+e^- \rightarrow \gamma e^+e^-$ (including $J/\psi \rightarrow \gamma e^+e^-$), respectively. Samples with backgrounds less than 1.0% are obtained [37]. The differences between data and MC for the efficiencies of pion and electron PID are about 1.0% and 1.2%, respectively, which are taken as systematic errors. Using the same control samples,

TABLE I: The fitted signal and background yields for $J/\psi \rightarrow \phi\eta$ (η'), η (η') $\rightarrow \pi^+\pi^-\pi^0$ (η), and ϵ^η ($\epsilon^{\eta'}$) is its selection efficiency.

Quantity	Value	
	η	η'
$N^\eta(N^{\eta'})$	3850 ± 73	1623 ± 44
$N_{\text{bkg}}^{\text{non-}\phi\eta}(N_{\text{bkg}}^{\text{non-}\phi\eta'})$	24 ± 8	49 ± 10
$N_{\text{bkg}}^{\text{non-}\phi}(N_{\text{bkg}}^{\text{non-}\phi})$	367 ± 43	22 ± 17
$N_{\text{bkg}}^{\text{non-}\eta}(N_{\text{bkg}}^{\text{non-}\eta'})$	88 ± 14	61 ± 12
ϵ^η ($\epsilon^{\eta'}$)	20.37%	20.89%

we estimate the uncertainty due to the requirement of E/p for the electron selection to be 3.5% (3.4%) for the η (η') case, and the uncertainty due to the requirement of E/p for pion selection in the η semileptonic decay is estimated to be 0.8%. The systematic uncertainty due to the requirements of ϕ and η (η') mass windows are estimated to be 1.4% and 0.04% (0.2%) by using the control sample of $J/\psi \rightarrow \phi\eta$ (η'), η (η') $\rightarrow \pi^+\pi^-\pi^0$ (η).

The uncertainty in the determination of the numbers of observed events for $J/\psi \rightarrow \phi\eta$ [$\eta \rightarrow \pi^+\pi^-\pi^0$ ($\pi^0 \rightarrow \gamma\gamma$)] and $J/\psi \rightarrow \phi\eta'$ [$\eta' \rightarrow \pi^+\pi^-\eta$ ($\eta \rightarrow \gamma\gamma$)] decays are estimated on the basis of earlier published results. The photon detection efficiency and its uncertainty are studied by three different methods in Ref [37]. The systematic error of photon detection is estimated to be 1.0% per photon. In the fit to the ϕ mass distribution, the mass resolution is fixed to the MC simulation; the level of possible discrepancy is determined with a smearing Gaussian, for which a non-zero σ would represent a MC-data difference in the mass resolution. The uncertainty associated with the difference determined in this way is 0.03% (0.06%) for the η (η') case. The systematic uncertainty due to the choice of parameterization for the shape of the non- $\phi\eta$ (η')-peaking background is estimated by varying the order of the polynomial in the fit; we find the relative changes on the η (η') signal yield of 1.3% (0.8%), which is taken as the uncertainty due to the background shapes. The systematic errors from π^0 (η) reconstruction from $\gamma\gamma$ decays is determined to be 1.0% per π^0 (η) by using a high purity control sample of $J/\psi \rightarrow \pi^0 p\bar{p}$ ($J/\psi \rightarrow \eta p\bar{p}$) decay [38]. The branching fractions for the π^0 and $\eta \rightarrow \gamma\gamma$ decays are taken from the PDG [29]. The uncertainties on the branching fractions are taken as a systematic uncertainty in our measurements. The total systematic error σ_η^{sys} ($\sigma_{\eta'}^{\text{sys}}$) on the ratio is 5.6% (7.4%) for η (η'), as summarized in Table II.

TABLE II: Summary of relative systematic errors for the determination of ratios of semileptonic over hadronic decays. The first nine lines are relevant for the semileptonic weak decay chain $J/\psi \rightarrow \phi\eta$ (η'), η (η') $\rightarrow \pi^+e^-\bar{\nu}_e$. The next five lines are relevant for the determination of the signal yield of the hadronic decay process $J/\psi \rightarrow \phi\eta$ (η'), $\eta \rightarrow \pi^+\pi^-\pi^0$ ($\eta' \rightarrow \pi^+\pi^-\eta$).

Sources	Sys. error (%)	
	η	η'
Requirement on N_{shower}	0.1	1.1
Requirement on P_{miss}	2.5	2.5
Signal model	1.0	5.0
Electron PID	1.2	1.2
Requirement on E/p for e	3.5	3.4
Requirement on E/p for π	0.8	-
ϕ mass window	1.4	1.4
η (η') mass window	0.0	0.2
Photon efficiency	2.0	2.0
π PID	1.0	1.0
Signal shapes for $\eta(\eta') \rightarrow \pi^+\pi^-\pi^0$ (η)	0.0	0.1
Background shape for $\eta(\eta') \rightarrow \pi^+\pi^-\pi^0$ (η)	1.3	0.8
π^0 (η) reconstruction	1.0	1.0
Cited $\mathcal{B}(\pi^0(\eta) \rightarrow \gamma\gamma)$	0.0	0.5
Total	5.6	7.4

V. RESULTS

The upper limit on the ratio of branching fractions of the semileptonic decay $\mathcal{B}(\eta \rightarrow \pi^+e^-\bar{\nu}_e + c.c.)$ over the hadronic decay $\mathcal{B}(\eta \rightarrow \pi^+\pi^-\pi^0)$ is calculated with

$$\frac{\mathcal{B}(\eta \rightarrow \pi^+e^-\bar{\nu}_e + c.c.)}{\mathcal{B}(\eta \rightarrow \pi^+\pi^-\pi^0)} < \frac{N_{\text{UL}}^\eta/\epsilon_\eta^{\text{SL}}}{N^\eta/\epsilon^\eta} \frac{\mathcal{B}(\pi^0 \rightarrow \gamma\gamma)}{(1 - \sigma_\eta)}, \quad (3)$$

where N_{UL}^η is the 90% upper limit of the observed number of events for $J/\psi \rightarrow \phi\eta$, $\phi \rightarrow K^+K^-$, $\eta \rightarrow \pi^+e^-\bar{\nu}_e$ decay, $\epsilon_\eta^{\text{SL}}$ is the MC determined efficiency for the signal channel, N^η is the number of events for the $J/\psi \rightarrow \phi\eta$, $\phi \rightarrow K^+K^-$, $\eta \rightarrow \pi^+\pi^-\pi^0$ ($\pi^0 \rightarrow \gamma\gamma$) decay, ϵ^η is the MC determined efficiency for the decay mode, and $\sigma_\eta = \sqrt{(\sigma_\eta^{\text{sys}})^2 + (\sigma_\eta^{\text{stat}})^2} = 5.9\%$, where σ_η^{sys} and $\sigma_\eta^{\text{stat}}$ are the total relative systematic error for the η case from Table II and the relative statistical error of N^η , respectively. For η' , $\sigma_{\eta'} = \sqrt{(\sigma_{\eta'}^{\text{sys}})^2 + (\sigma_{\eta'}^{\text{stat}})^2} = 7.9\%$.

The relative statistical error of N^η ($N^{\eta'}$) is 1.9% (2.7%). We also obtain the upper limit on the ratio of $\mathcal{B}(\eta' \rightarrow \pi^+e^-\bar{\nu}_e + c.c.)$ to $\mathcal{B}(\eta' \rightarrow \pi^+\pi^-\eta)$ by replacing η and $\mathcal{B}(\pi^0 \rightarrow \gamma\gamma)$ with η' and $\mathcal{B}(\eta \rightarrow \gamma\gamma)$, respectively, in Eq. (3). Since only the statistical error is considered when we obtain the 90% upper limit of the number of events, to be conservative, N_{UL}^η and $N_{\text{UL}}^{\eta'}$ are shifted up by one sigma of the additional uncertainties (σ_η or $\sigma_{\eta'}$).

Using the numbers in Table III, the upper limits on the ratios $\frac{\mathcal{B}(\eta \rightarrow \pi^+e^-\bar{\nu}_e + c.c.)}{\mathcal{B}(\eta \rightarrow \pi^+\pi^-\pi^0)}$ and $\frac{\mathcal{B}(\eta' \rightarrow \pi^+e^-\bar{\nu}_e + c.c.)}{\mathcal{B}(\eta' \rightarrow \pi^+\pi^-\eta)}$ are obtained at the 90% C.L. of 7.3×10^{-4} and 5.0×10^{-4} , respectively.

TABLE III: The numbers used in the calculations of the ratios in Eq. (3), where $N_{UL}^\eta(N_{UL}^{\eta'})$ is the upper limit of the signal events at the 90% C.L., $\epsilon_{\eta}^{SL}(\epsilon_{\eta'}^{SL})$ is the selection efficiency, $N^\eta(N^{\eta'})$ is the number of the events of $J/\psi \rightarrow \phi\eta(\eta')$, $\phi \rightarrow K^+K^-$, $\eta \rightarrow \pi^+\pi^-\pi^0$ and $\pi^0 \rightarrow \gamma\gamma$ ($\eta' \rightarrow \pi^+\pi^-\eta$ and $\eta \rightarrow \gamma\gamma$), $\epsilon^\eta(\epsilon^{\eta'})$ is its selection efficiency, $\sigma_\eta^{\text{stat}}(\sigma_{\eta'}^{\text{stat}})$ is the relative statistical error of $N^\eta(N^{\eta'})$, and $\sigma_\eta(\sigma_{\eta'})$ is the total relative error.

Quantity	Value	
	η	η'
$N_{UL}^\eta(N_{UL}^{\eta'})$	2.36	1.59
$\epsilon_{\eta}^{SL}(\epsilon_{\eta'}^{SL})$	17.9%	17.4%
$N^\eta(N^{\eta'})$	3850 ± 73	1623 ± 44
$\epsilon^\eta(\epsilon^{\eta'})$	20.37%	20.89%
$\sigma_\eta^{\text{stat}}(\sigma_{\eta'}^{\text{stat}})$	1.9%	2.7%
$\sigma_\eta(\sigma_{\eta'})$	5.9%	7.9%

VI. SUMMARY

A search for the semileptonic weak decay modes $\eta(\eta') \rightarrow \pi^+e^-\bar{\nu}_e$ has been performed for the first time in the process of $J/\psi \rightarrow \phi\eta(\eta')$ using the $(225.3 \pm 2.8) \times 10^6$ J/ψ events measured at BESIII. We find no signal yields for the semileptonic weak decays of η and η' . The upper limits at the 90% C.L. are 7.3×10^{-4} and 5.0×10^{-4} for the ratios of semileptonic over hadronic decay modes $\frac{\mathcal{B}(\eta \rightarrow \pi^+e^-\bar{\nu}_e + c.c.)}{\mathcal{B}(\eta \rightarrow \pi^+\pi^-\pi^0)}$ and $\frac{\mathcal{B}(\eta' \rightarrow \pi^+e^-\bar{\nu}_e + c.c.)}{\mathcal{B}(\eta' \rightarrow \pi^+\pi^-\eta)}$, respectively. The advantage of measuring the ratios instead of the branching fractions of the semileptonic weak decays is that many uncertainties cancel. Using the hadronic branching fraction values of $\eta \rightarrow \pi^+\pi^-\pi^0$

and $\eta' \rightarrow \pi^+\pi^-\eta$ as listed by PDG [29], we determine the semileptonic decay rates to be $\mathcal{B}(\eta \rightarrow \pi^+e^-\bar{\nu}_e + c.c.) < 1.7 \times 10^{-4}$ and $\mathcal{B}(\eta' \rightarrow \pi^+e^-\bar{\nu}_e + c.c.) < 2.2 \times 10^{-4}$ at the 90% C.L..

Acknowledgments

The BESIII collaboration thanks the staff of BEPCII and the computing center for their hard efforts. This work is supported in part by the Ministry of Science and Technology of China under Contract No. 2009CB825200; National Natural Science Foundation of China (NSFC) under Contracts Nos. 10625524, 10821063, 10825524, 10835001, 10935007, 11125525, 11061140514; Joint Funds of the National Natural Science Foundation of China under Contracts Nos. 11079008, 11179007, 11179014; the Chinese Academy of Sciences (CAS) Large-Scale Scientific Facility Program; CAS under Contracts Nos. KJCX2-YW-N29, KJCX2-YW-N45; 100 Talents Program of CAS; Istituto Nazionale di Fisica Nucleare, Italy; Ministry of Development of Turkey under Contract No. DPT2006K-120470; U. S. Department of Energy under Contracts Nos. DE-FG02-04ER41291, DE-FG02-94ER40823; U.S. National Science Foundation; University of Groningen (RuG) and the Helmholtzzentrum fuer Schwerionenforschung GmbH (GSI), Darmstadt; WCU Program of National Research Foundation of Korea under Contract No. R32-2008-000-10155-0; German Research Foundation DFG within the Collaborative Research Center CRC1044.

-
- [1] P. Fayet, Phys. Lett. B **84**, 421 (1979); P. Fayet and J. Kaplan, Phys. Lett. B **269**, 213 (1991); B. McElrath, Phys. Rev. D **72**, 103508 (2005).
- [2] P. Fayet, Phys. Rev. D **74**, 054034 (2006).
- [3] P. Fayet, Phys. Rev. D **75**, 115017 (2007).
- [4] M. Ablikim *et al.* (BES Collaboration), Phys. Rev. Lett. **97**, 202002 (2006); Phys. Rev. Lett. **100**, 192001 (2008).
- [5] R. Balest *et al.* (CLEO Collaboration), Phys. Rev. D **51**, 2053 (1995).
- [6] P. Rubin *et al.* (CLEO Collaboration), Phys. Rev. D **75**, 031104 (2007); O. Tajima *et al.* (Belle Collaboration), Phys. Rev. Lett. **98**, 132001 (2007).
- [7] H. B. Li and S. H. Zhu, Chinese Physics C **36**, 932(2012).
- [8] P. Singer, Phys. Rev. **139**, B483 (1965).
- [9] S. Weinberg, Phys. Rev. **112**, 1375 (1958).
- [10] L. B. Okun, I. S. Tsukerman, Sov. Phys. JETP **20**, 232 (1965).
- [11] P. Herczeg, in *Proceedings of the Conference on the Intersections Between Particle and Nuclear Physics*, edited by W. T. H. van Gers, AIP Conf. Proc. No. **243**, 654 (1992).
- [12] H. Neufeld, H. Rupertsberger, Z. Phys. C **68**, 91(1995).
- [13] A. Branmon and E. Shabalin, Phys. Atom. Nucl. **58**, 1931(1995); Yad. Fiz. **58**, 2041(1995).
- [14] J. N. Ng, in *Proceedings of the Conference on Particle Production Near Threshold*, edited by H. Nann and E. J. Stephenson, AIP Conf. Proc. No. **221**, 26 (1990).
- [15] W. Lucha, H. Pietschmann, H. Rupertsberger, and F. F. Schöberl, Phys. Rev. D **46**, 2255 (1992).
- [16] D. Scora and K. Maltman, Phys. Rev. D **51**, 132 (1995).
- [17] E. Shabalin, Physica Scripta. **T99**, 104(2002).
- [18] T. D. Lee, Phys. Rev. D **8**, 1226 (1970).
- [19] S. Weinberg, Phys. Rev. Lett. **37**, 657 (1976).
- [20] S. M. Barr and A. Masiero, Phys. Rev. Lett. **58**, 187 (1987).
- [21] D. Wyler, in *Proceedings of Int. Workshop on Rare decays of light mesons*, Gif-sur-Yvette, France, 1990 (Editions Frontières, Gif-sur-Yvette, France, 1990) p. 125.
- [22] P. Herczeg, in *Proceedings of the workshop on the Production and Decay of Light Mesons*, edited by P. Fleury, (Singapore: World Scientific) p. 16 (1988).
- [23] P. Herczeg, Prog. Part. Nucl. Phys. **46**, 413 (2001).
- [24] M. Ablikim *et al.* (BESIII Collaboration), Chinese Phys. C **36**, 915(2012).
- [25] M. Ablikim *et al.* (BESIII Collaboration), Nucl. Instrum.

- Meth. A **614**, 345 (2010).
- [26] S. Agostinelli *et al.* (GEANT4 Collaboration), Nucl. Instrum. Meth. A **506**, 250 (2003).
- [27] S. Jadach, B. F. L. Ward and Z. Was, Comput. Phys. Commun. **130**, 260 (2000); S. Jadach, B. F. L. Ward and Z. Was, Phys. Rev. D **63**, 113009 (2001).
- [28] D. J. Lange, Nucl. Instrum. Meth. A **462**, 152 (2001).
- [29] J. Beringer *et al.* (Particle Data Group), Phys. Rev. D **86**, 010001 (2012).
- [30] J. C. Chen, G. S. Huang, X. R. Qi, D. H. Zhang, and Y. S. Zhu, Phys. Rev. D **62**, 034003 (2000).
- [31] W. D. Li, H. M. Liu *et al.*, in *Proceedings of CHEP06, Mumbai, India*, 2006 edited by Sunanda Banerjee (Tata Institute of Fundamental Research, Mumbai, 2006).
- [32] J. Conrad, O. Botner, A. Hallgren and C. Perèz de los Heros, Phys. Rev. D **67**, 012002 (2003); <http://polepp.googlecode.com/svn/tags/POLEPP-1.1.0>.
- [33] G. J. Feldman and R. D. Cousins, Phys. Rev. D **57**, 3837 (1998).
- [34] F. von Hippel and C. Quigg, Phys. Rev. D **5**, 624, (1972); J. Blatt and V. Weisskopf, *Theoretical Nuclear Physics* (John Wiley & Sons, New York, 1952).
- [35] J. E. Gaiser, Ph.D. thesis, [Stanford University, Report No. SLAC-R-255, 1982 (unpublished)]; M. J. Oreglia, Ph.D. thesis, [Stanford University, Report No. SLAC-R-236, 1980 (unpublished)]; T. Skwarnicki, Ph.D. thesis, [Cracow University of Technology, Report No. DESY-F-31-86-02, 1986 (unpublished)].
- [36] C. C. Chang *et al.* (E580 Collaboration), Phys. Rev. D **29**, 1888 (1984); D. Barberis *et al.* (WA102 Collaboration), Phys. Lett. B **436**, 204 (1998).
- [37] M. Ablikim *et al.* (BESIII Collaboration), Phys. Rev. D **83**, 112005 (2011).
- [38] M. Ablikim *et al.* (BESIII Collaboration), Phys. Rev. Lett. **105**, 261801 (2010).